How Lithography Affects Etch Simulations for Lithography Engineers

Robert Jones, Chris A. Mack, and Jeffrey Byers, KLA-Tencor Corporation

We introduce the concept of etch simulations for lithography engineers. Traditional lithographic simulations begin with a design layout and model the optical and chemical processes involved in reproducing the design as a 3-dimensional photoresist pattern. What we are really after, however, is information about the pattern, as it would appear in silicon.

Introduction

The goal of virtually every lithography process step is to transfer a pattern into the substrate. For some years, optical lithography simulation has been an accepted part of the manufacturing process. But lithography simulations alone leave us one step short of our desired goal. The combination of an optical lithography simulator and an etch simulator, however, allows us to simulate the entire pattern transfer process and to determine the impact of the final resist profile shape on the quality of the etched pattern in the substrate.

To minimize the complexity of the etch simulations, we have necessarily lumped all of the physics into a few simple parameters —the kinds of parameters that can be obtained from a series of cross-sectional SEM images. We do not attempt to calculate etch rates from plasma chemistry, ion energies, and film stack materials. Instead, we take measured etch rates for each material in the film stack, and treat the etched surface as an advancing wave front propagating with a material and directionally dependent speed. We take the flux of incoming ions to be a simple distribution—either uniform and purely vertical, or with a Gaussian profile in the flux angle about the vertical. Using the ion flux information, we compute visibility and shadowing effects—materials exposed to the ion source directly etch faster than those hidden from the source. We also treat the nonlinear angular dependence of the physical sputtering yield with a single, materially dependent, fitting parameter.

Given these input parameters, we treat the etch problem as that of an advancing wave front which obeys a Hamilton-Jacobi equation. We compute a "Hamiltonian" based on the input parameters and the already calculated resist profile, and advance the solution consistent with Sethian's[1] level set formulation. Finally, we extract relevant etch metrology from the position of the simulated wave front, or etch profile.

By taking several sets of etch rate data, ion spread, and faceting parameters, we can model real world plasma chemistries which vary over the course of a full etch process. Using a set of cross-sectional SEM images from a series of wafers at various stages of the etch process, we extract our model input parameters as we fit our simulated profiles to the experimental data. Once we have a tuned etch model, corresponding to a full etch process, we are free to vary any lithographic input or even the etch model parameters. With this technique, we can consider both the effect of varying lithographic inputs on final etch profiles and etch process windows, and different etch processes and chemistries as correlated to etch model inputs.

Etch model and input parameters

As we have already said, the model describes the etched surface as wave front propagating with a material and position dependent speed. The analysis here is similar to that of advancing flame fronts. All of the physics is contained in the material etch rates, r_h and r_v, a faceting parameter, A, related to physical sputtering, and a masking function, M(x, y, z), which describes the surface visibility from the ion source. The horizontal and vertical

etch rates, r_h and r_v, are material dependent and, as such, vary as a function of depth into the film stack. The masking function modifies the speed of the wave front, and, therefore, the etch profile to allow shadow-like effects. Including the angular distribution of the ions allows predictions of iso-dense etch bias. The masking function, etch rates, and faceting parameter are combined into an overall speed function for the advancing wave front. The speed function is extendable to include additional physical effects such as scattering, re-emission, etc. Real-world etching effects, such as undercutting, shadowing, and tapering are seen in the predicted profiles.

We begin by embedding the initial resist profile as the zero level set of a higher dimensional function $\varphi(x, z)$, where we are taking the vertical axis as z, and the horizontal axis as x. We set:

$$\varphi(x,z) = \pm d$$

where d is the distance from the point (x,z) to the surface. That is to say, the value stored at every point in the volume is just the (shortest) distance from that point to the surface. In Figure 1 we see a regular 2D resist profile (line) over a silicon substrate. Negative values correspond to points that have already been developed/etched away. Positive values indicate remaining material.

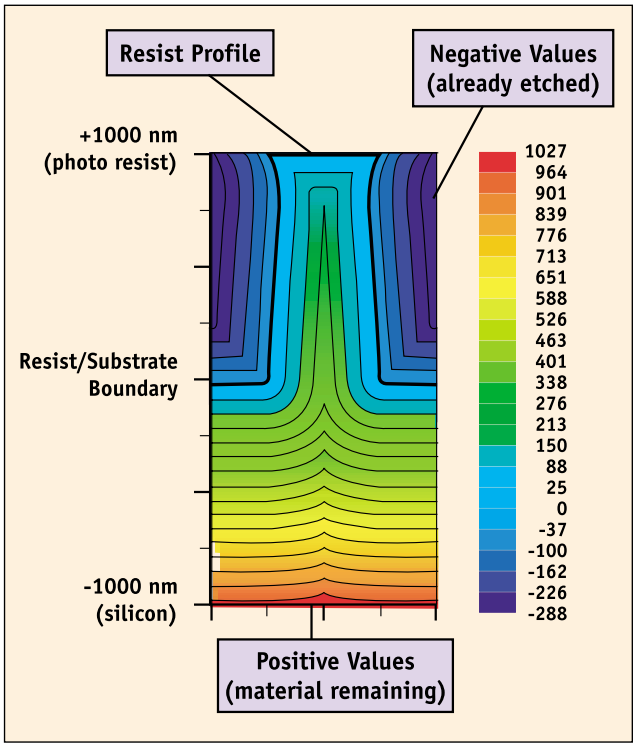

Figure 1. A contour plot of the Level-Set distance function φ(x,z).

We then treat the surface as a propagating wave front, following the analysis originally developed by Sethian and Osher[2] to model advancing flame fronts. We solve the Hamilton-Jacobi equation, which gives the evolution of the surface. In two-dimensions this is just:

$$\frac{\partial \varphi}{\partial t} + H\left(\frac{\partial \varphi}{\partial x}, \frac{\partial \varphi}{\partial z}\right) = 0$$

where, in this case, the "Hamiltonian" is given by:

$$H\left(\frac{\partial \varphi}{\partial x}, \frac{\partial \varphi}{\partial z}\right) = F(x,z)\left|\nabla \varphi\right|$$

where F is the speed function for the advancing surface, given in 2-dimensions by:

$$F(x,z) = r_h + (r_v - r_h)V(x,z,\alpha)(1 + A\sin^2\theta)\cos\theta$$

This says that the function $\varphi(x, z)$ moves in a direction normal to itself with a speed that depends on the angle between the surface normal and the positive z-axis. The first term is the isotropic part; it is the directionless speed of the front, which is equal to the horizontal etch rate of the material. The second part is the anisotropic etch rate. It depends on the angle between the surface normal and the z-axis and on the visibility of the ion source from each surface point. The angle θ is measured between the surface normal and the z-axis, and is given by:

$$\cos\theta = \frac{\varphi_z}{\left|\nabla \varphi\right|}$$

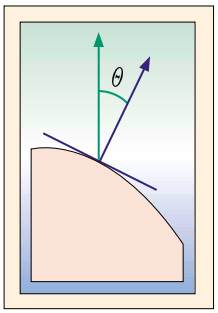

Figure 2. Measuring angles.

$V(x,z,\alpha)$ is the visibility function, which gives the fraction of the cone defined by the half angle α which is open to the ion source above. If the source is completely open, e.g., in a large open area $V(x,z,\alpha) = 1$, and if the source is completely blocked, e.g., below an undercut layer of material, then $V(x,z,\alpha) = 0$. Between these extremes, V is defined as:

$$V(x,z,\alpha) = \frac{1}{\sqrt{2\pi}}\int_{-1}^{1} \delta_{vis}(x,z,\alpha\, t)\exp\left(\frac{-9t^2}{2\alpha^2}\right) dt$$

where δ_{vis} is a visibility delta function defined so that $\delta_{vis}(x,z,\alpha) = 1$ when the source is visible along the ray from the point (x, z) at an angle α with the vertical,

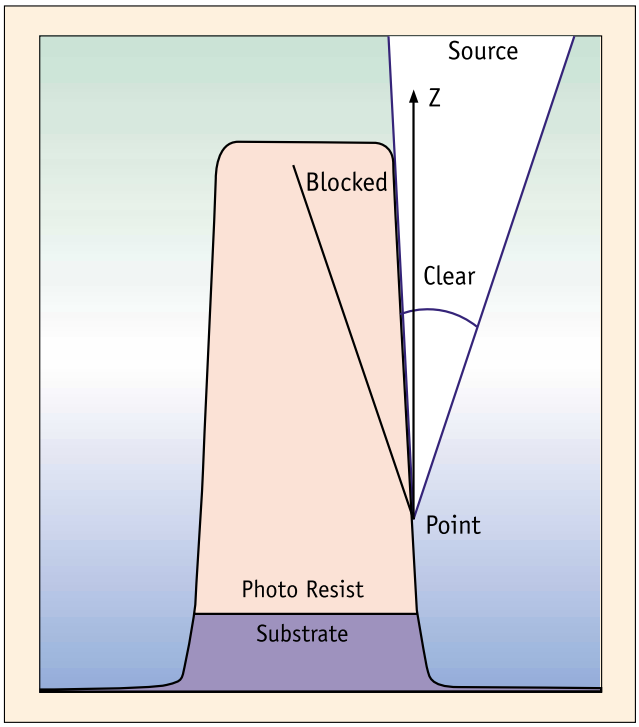

Figure 3. Visibility Cone.

and is zero otherwise. Using this definition implies that the incoming ion flux angles are normally distributed about the vertical with a standard deviation of 3α.

Tuning the simulation to experiment

The simulation produces several outputs, namely, an etch profile and its associated metrology—after etch CD, side wall angle, resist loss, etch depth, etc. But, as is usual, we are primarily concerned with the etch profile. Let's consider the case of an actual two-dimensional etch problem. We'll run a set of isolated and dense lines at 275 nm target width. We tune the lithography simulator to match actual data obtained from experiments at SEMATECH[3]. We extract the etch simulation input parameters from cross sectional SEMs of the etched wafers at various stages of completion. The process was an older one, but it is still a useful test of the etch simulator. We consider data from series of wafers exposed on a 248 nm stepper with a numerical aperture of 0.53 and a partial coherence of 0.74. The wafers had a 230 nm poly-silicon layer over a thin oxide layer. The poly was coated with 740 nm of APEX-E photoresist over 63 nm of Brewer CD11 ARC for lithography.

The target etch process consisted of four etch stages—a 10 second break through etch to get through the BARC, a 60 second main etch, a 36 second over etch, and a 10 second strip. The break through and main etch stages produced a fair amount of deposition, taking the resist profile from a 260 nm width to a 350 nm width. The over etch trimmed this back to the 310 nm range. Deposition is treated in the model as a negative horizontal etch rate. The break through and main etch stages also contained a fair amount of physical sputtering; this manifested as a faceting of the resist near the top. The full set of etch parameters used (for all four stages) is given in Table 1.

In the following series of images, we compare the simulated etch profiles to actual cross sections at various stages of completion. Figure 4 shows a break through etch which has cut through the ARC layer and penetrated into the silicon only slightly (~25 nm). The resist lost 109 nm of thickness, gained 38 nm of width, and was faceted at the top. The overall shape of the simulated profile on the right is consistent with the cross section shown at the left, and matches the after etch CD to within a few nanometers.

In the next image, Figure 5, we see a simulation of the main etch stage. Deposition has increased the width of the profile to 357 nm at the base. The poly layer has been completely cut through, and the top of the oxide etch stop layer is seen in at the base of the simulated profile.

Etch Time(s)	Ion Spread (deg)	Material	Vertical Etch Rate (nm/s)	Horizontal Etch Rate (nm/s)	Faceting Parameter
10	10	APEX E	10.66	-2.6	0.5
		Brewer ARC CD11	10.52	-1.7	0
		Polysilicon	4.28	0	0
		Silicon Dioxide	0	0	0
60	10	APEX E	0.3	-0.3	0.5
		Brewer ARC CD11	3.4	-0.25	0
		Polysilicon	3.4	-0.2	0
		Silicon Dioxide	0	0	0
36	10	APEX E	0.65	0.6	0
		Brewer ARC CD11	2.5	0.7	0
		Polysilicon	2.5	0.7	0
		Silicon Dioxide	0	0	0
10	10	APEX E	30	30	0
		Brewer ARC CD11	30	30	0
		Polysilicon	0	0	0
		Silicon Dioxide	0	0	0

Table 1. Full set of etch parameters for target etch process.

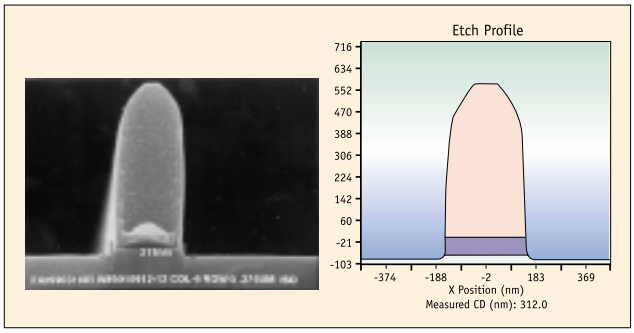

Figure 4. Break through etch for isolated 275 nm lines.

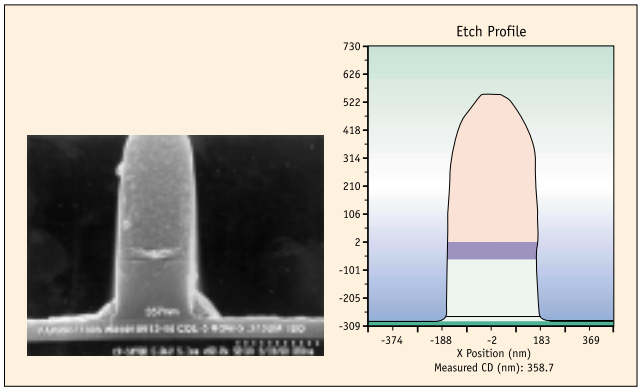

Figure 5. Main etch for isolated 275 nm lines.

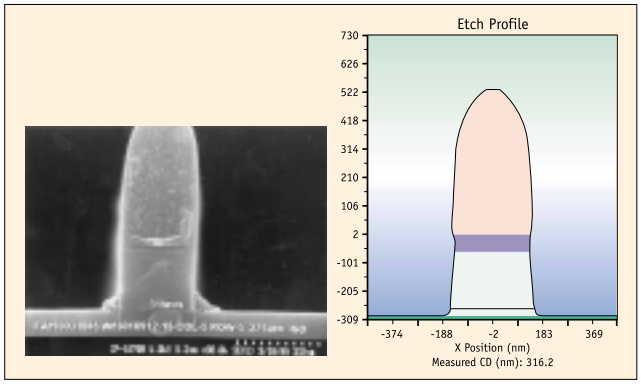

Figure 6. Over etch for isolated 275 nm lines.

After the over etch stage, the profiles have been trimmed back some 40 nm near the base, as shown in Figure 6. The process also produced some undercutting of the resist. This will be more pronounced in the dense lines.

Finally, in Figure 7, we see the results of the simulation after strip. The sidewalls are showing a little more slant in the simulated profile than in the experimental data but the CD match was quite good.

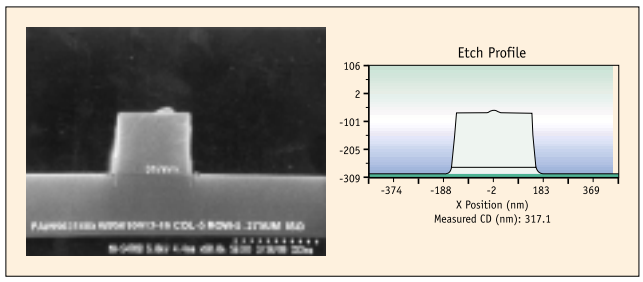

Figure 7. Isolated 275 nm lines after resist strip.

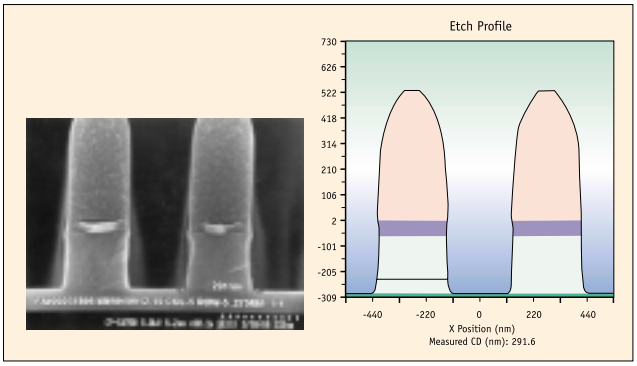

Figure 8. Dense 275 nm lines after main etch.

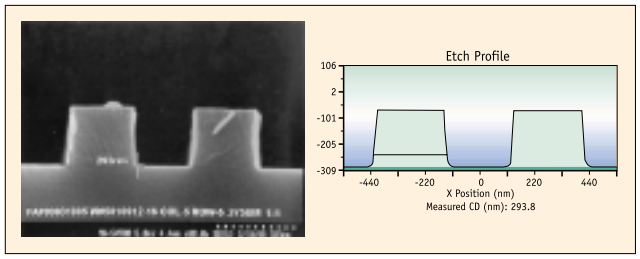

Figure 9. Dense 275 nm lines after resist strip.

In Figures 8 and 9, we see the same etch simulation for dense lines. The only parameter changed in the simulation is the pitch of the mask, which has been reduced from 2500 nm to 550 nm. The first image shows the results of simulation through the over etch stage. Undercutting of the resist is more pronounced here than in the isolated lines.

Simulation analysis and results

Given this tuned model for the etch process, we are now free to conduct a series of numerical experiments which employ the predictive value of the model. As with all of our etch simulations, we are trying to answer the question, "How does the lithography, through the resist profile, affect after etch CDs?" We begin by running a focus exposure matrix for both the isolated

and dense lines. The resist profiles and corresponding etch profiles seen in the FE matrices are shown in Table 2 below. The resist profiles span a large range of shape and size; the etch profiles show a smaller range of variation. This fact becomes more apparent when we look at the process window.

We compute a CD process window, as seen in Figure 10, by demanding the final CD lie within ±10 % of the desired CD. Overlapping the results for the isolated and dense lines, and considering the lithography and etch results separately, we find that the etch process has increased the process latitude. The process window for the dense lines gains in exposure latitude, while the isolated line process window gains focal latitude. The result is an enlarged process window after etch, with a best focus shifted from –0.36 microns to –0.26 microns, and a best exposure shifted from 8.16 to 8.02 mJ/cm^2.

As seen in Figure 11, the exposure latitude versus depth of focus curves are also pushed out almost uniformly from their before etch positions, indicating greater process latitude after etch.

As another example of the kinds of useful simulations that can be performed with our etch model, consider a series of simulations in which we vary the pitch of the mask from 550 nm to 2500 nm. The endpoints are anchored by our tuned modeling results, and the remaining points are predicted by simulation alone. The Feature Width versus Pitch curve, shown in Figure 12, after etch follows the same general trend as the before etch curve, but with greater iso-dense bias. Before etch, the iso-dense bias was only about 15 nm, while after etch it was about 25 nm.

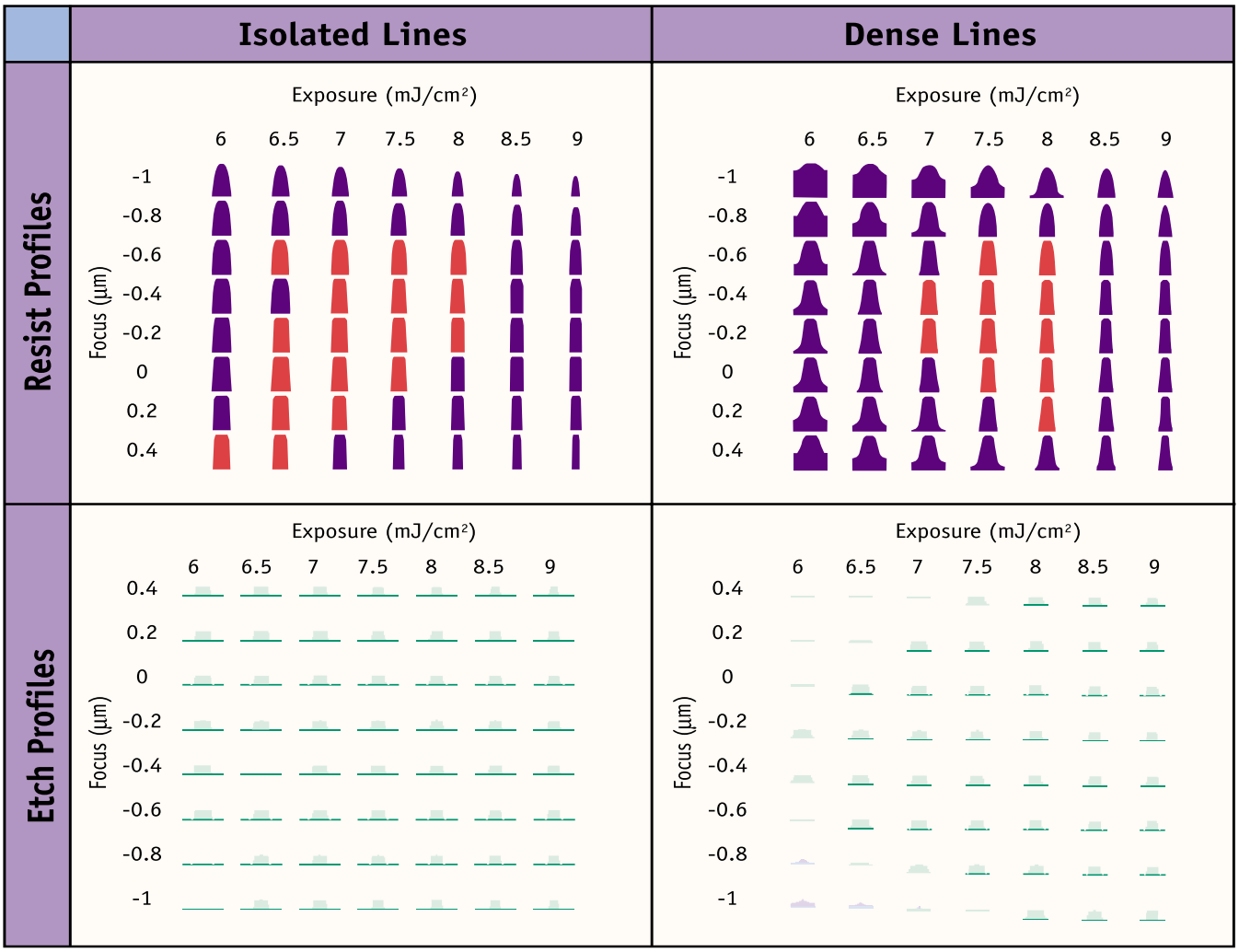

Table 2. Focus exposure matrix of isolated and dense lines.

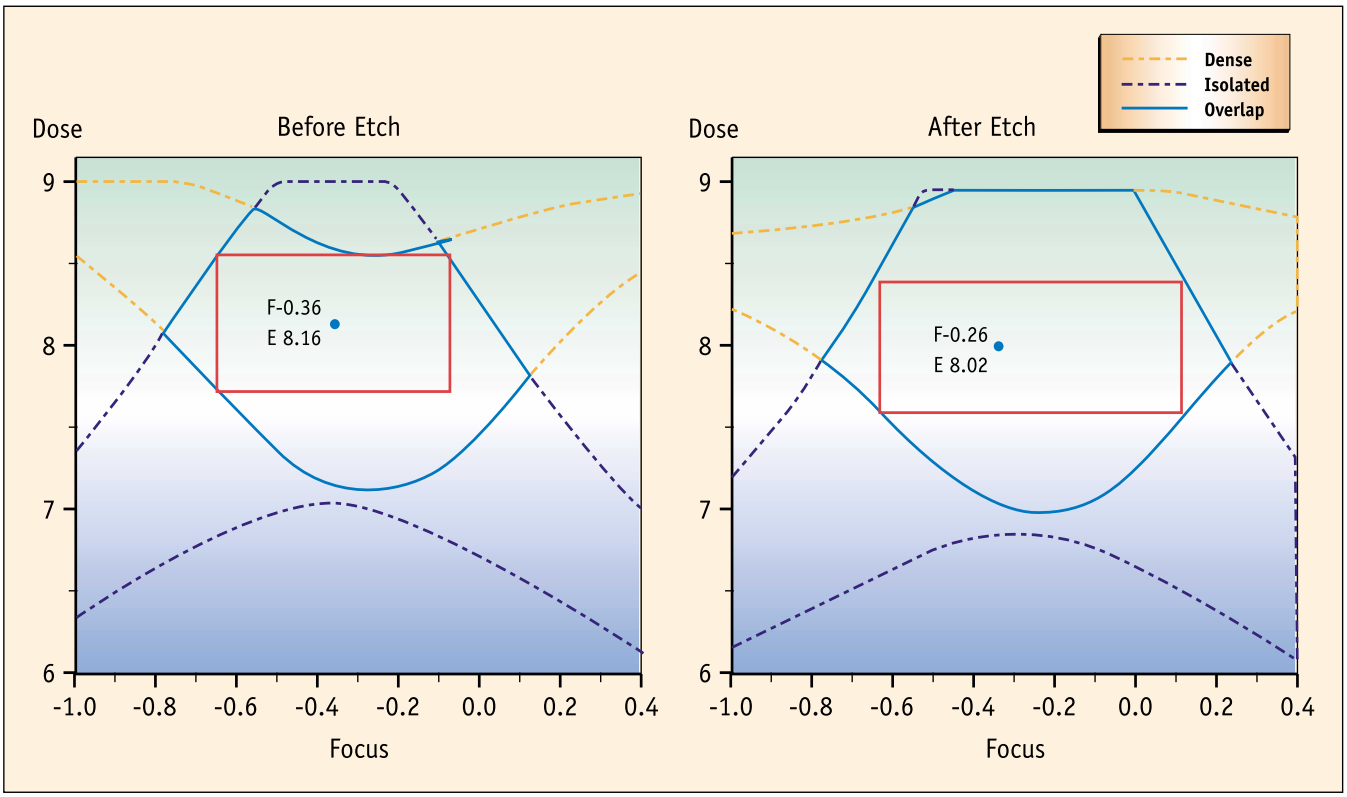

Figure 10. CD Process windows before and after etch.

3-Dimensional simulations

So far, all the simulations shown in this paper have been 2-dimensional line-and-space patterns. The etch model, however, extends naturally to 3-dimensions with no additional parameters. In this case, the horizontal etch rate means the uniform etch rate in the x and y planes. The ion spread parameter becomes the half angle of the 3-dimensional cone of visibility rather than a 2-dimensional triangle. The other parameters have no alternate interpretation. Using the same set of parameters presented above, we will now consider line end shortening in a T-shaped mask. The mask is a T made of 275 nm

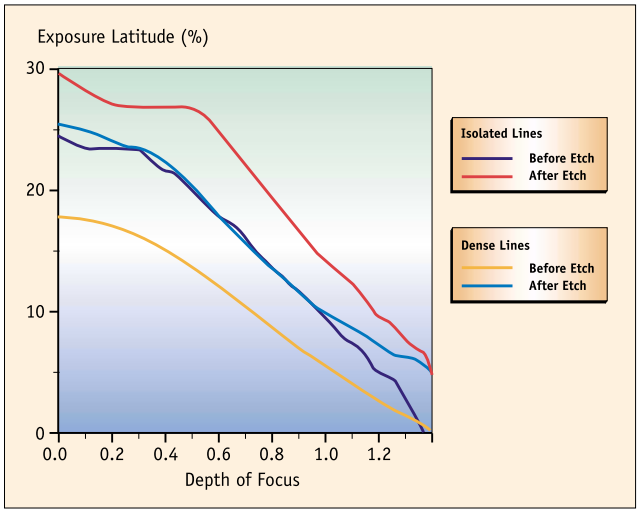

Figure 11. Exposure latitude versus depth of focus before and after etch.

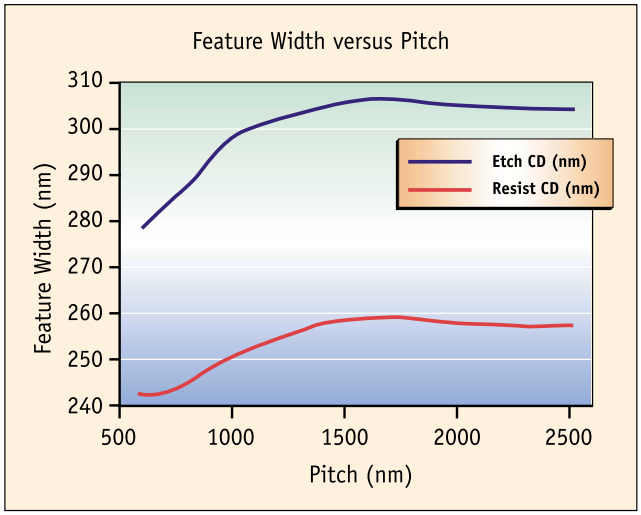

Figure 12. Feature width versus pitch.

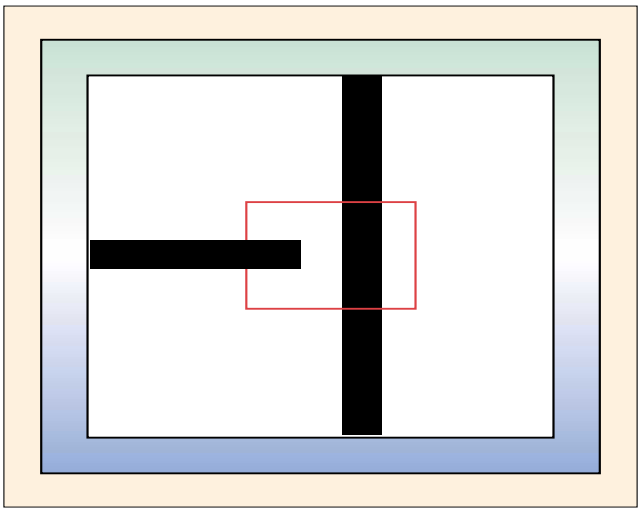

Figure 13. A chrome-on-glass line end shortening tee mask with a box showing the simulated region.

lines with a 275 nm gap between them as shown in Figure 13. The resist profile and etch profile (after strip) calculated from this mask are shown in Figures 14 and 15.

The plane cutting through the profile indicates the metrology plane (where measurements are made). If we consider the Aerial Image alone, the estimated CD of the gap is 318 nm. A full resist simulation gives the gap as 325 nm. But the etch simulation gives it at 310 nm. We might try to correct this pullback with serifing. In the chart below, we plot the gap width versus serif size for various serif sizes. We note that a serif size of around 85 nm would be required to size the gap to 275 nm according to the etch simulation. Resist simulation alone would overestimate the size of the gap by nearly 16 nm. Using the Aerial Image CD alone, a common technique in OPC engines, the gap width would be undersized by more than 21 nm.

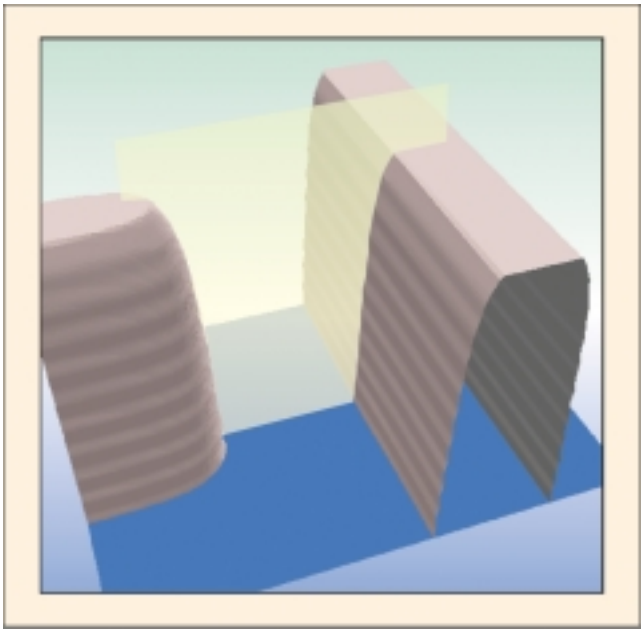

Figure 14. 3D resist profile for a line end shortening tee mask.

Conclusions and future work

We have seen in this paper a simplified model for etch processing. The model takes only a few simple inputs, yet yields many powerful and interesting results. Combined with an optical lithography simulator, we can now simulate the entire pattern transfer process. We can tune the model to match experimental data for a wide range of etch processes, and use the predictive value of the model to simulate many lithographic and etch processing conditions. The usefulness of the model to the lithographer will come foremost with the ability to optimize a lithographic process to obtain desired after etch results, but also with the instructive value the model has for lithographers trying to understand etch processing and its limitations. While we have not detailed the use of the model to simulate bilayer resist processes, such an application is straightforward.

This model essentially represents the most basic form an etch model can take while still producing useful results. There is, therefore, much room for additional physical effects to be added to the model. The first, and

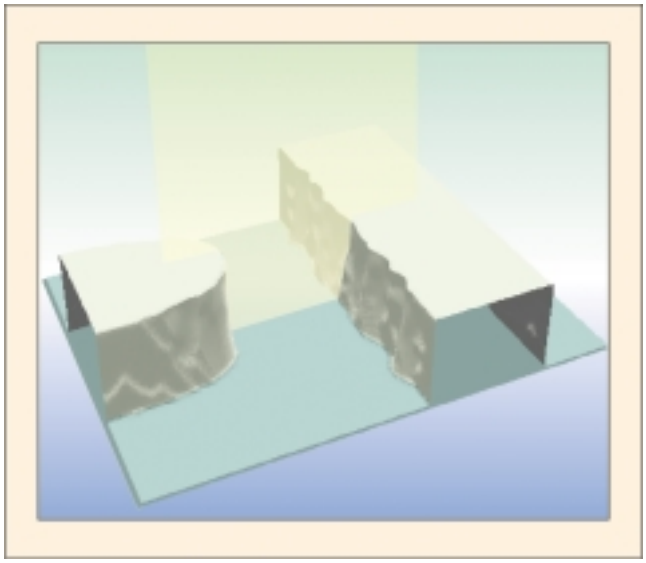

Figure 15. 3D etch profile (after strip) for a line end shortening tee mask.

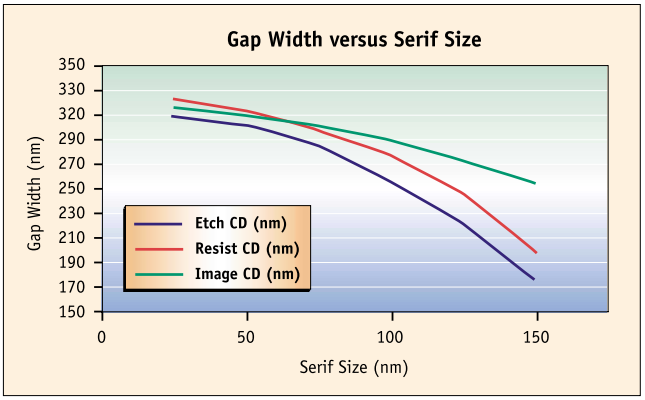

Figure 16. Simulations of gap width versus serif size on a line end shortening tee mask.

most obvious of these, is automatic tuning of etch parameters in the model to match cross-sectional SEMs. We can also imagine calculating the etch rates from more basic physical data. We can also imagine a kind of feed-forward process control being developed with this kind of etch model, where we keep the etch process constant, and alter the lithography to produce better after etch results.

Acknowledgements

The authors would like to thank Mark Smith and William Howard at KLA-Tencor for valuable technical assistance, Jeff Austell at KLA-Tencor for software development, and Danny Miller and David Stark at SEMATECH for providing SEM data and useful discussions. Partial funding for this research was provided by NIST through grant #70NANB8H4067.

References

1. James A. Sethian and David Adalsteinson, IEEE Trans. Semi. Manuf. 10, 167 (1997).
2. Stanley Osher and James A. Sethian, J. Comp. Phys. 79, 12-49 (1988).
3. Danny Miller and David Stark, SEMATECH, Private Communication (2002).

A version of this article was originally published in the 2002 SPIE Microlithography proceedings 4691, SPIE Microlithography Conference, March 3-8, 2002, Santa Clara, California, USA.